European Radiology (2019) 29:4123–4132
https://doi.org/10.1007/s00330-018-5838-8

EDITORIAL

Diffusion-weighted imaging and diffusion tensor imaging as adjuncts to conventional MRI for the diagnosis and management of peripheral nerve sheath tumors: current perspectives and future directions

Alexander T. Mazal[1] · Oganes Ashikyan[1] · Jonathan Cheng[2] · Lu Q. Le[3] · Avneesh Chhabra[1]

Received: 28 July 2018 / Revised: 29 September 2018 / Accepted: 17 October 2018 / Published online: 7 December 2018

Abstract

Peripheral nerve sheath tumors (PNSTs) account for ~5% of soft tissue neoplasms and are responsible for a wide spectrum of morbidities ranging from localized neuropathy to fulminant metastatic spread and death. MR imaging represents the gold standard for identification of these neoplasms, however, current anatomic MR imaging markers do not reliably detect or differentiate benign and malignant lesions, and therefore, biopsy or excision is required for definitive diagnosis. Diffusion-weighted MR imaging (DWI) serves as a useful tool in the evaluation and management of PNSTs by providing functional information regarding the degree of diffusion, while diffusion tensor imaging (DTI) aids in determining the directional information of predominant diffusion and has been shown to be particularly useful for pre-operative planning of these tumors by delineating healthy and pathologic fascicles. The article focuses on these important neurogenic lesions, highlighting the current utility of diffusion MR imaging and future directions including computerized radiomic analysis.

Key Points

- *Anatomic MRI is moderately accurate in differentiating benign from malignant PNST.*
- *Diffusion tensor imaging facilitates pre-operative planning of PNSTs by depicting neuropathy and tractography.*
- *Radiomics will likely augment current observer-based diagnostic criteria for PNSTs.*

Keywords Peripheral nerves · Nerve sheath neoplasms · Diagnostic techniques, neurological · Diffusion magnetic resonance imaging · Diffusion tensor imaging

Abbreviations

2D	2-dimensional
3D	3-dimensional
BPNST	Benign peripheral nerve sheath tumor
CE-T1W	Contrast-enhanced T1W image with fat suppression
CNRV	Contrast-to-noise ratio
F18 FDG-PET	Fluorine-18 fluorodeoxyglucose positron emission tomography
FA	Fractional anisotropy
fsPDW	Fat-saturated proton density weighted
fsT2W	Fat-suppressed T2W
IVIM	Intravoxel incoherent motion
MD	Mean diffusivity
MIP	Maximum intensity projection
MPNST	Malignant peripheral nerve sheath tumor
MRN	MR neurography
NF1	Neurofibromatosis type I
NF2	Neurofibromatosis type II
PNST	Peripheral nerve sheath tumor
PSIF	Reversed fast imaging in steady-state free precession

✉ Avneesh Chhabra
avneesh.chhabra@utsouthwestern.edu

[1] Department of Radiology, UT Southwestern Medical Center, Dallas, TX 75022, USA

[2] Department of Plastic Surgery, UT Southwestern Medical Center, Dallas, TX, USA

[3] Department of Dermatology and Simmons Comprehensive Cancer Center, UT Southwestern Medical Center, Dallas, TX, USA

SHINKEI	Nerve sheath signal increased with inked rest-tissue rapid acquisition of relaxation enhancement imaging
SNR	Signal-to-noise ratio
SPAIR	Spectral attenuated inversion recovery
STIR	Short TI inversion recovery
T	Tesla
T1W	T1-weighted
T2W	T2-weighted
TSE	Turbo spin echo

Introduction

PNSTs are soft tissue neoplasms of Schwann cell and/or perineurial cell origin. They are responsible for a wide spectrum of morbidities ranging from localized symptoms such as pain and motor/sensory impairment to fulminant metastatic spread and death, depending on the local invasive behavior and malignant transformative potential of the lesion [1]. Early diagnosis and treatment of these lesions is essential for the prevention of serious sequelae [2]. MRI currently represents the gold standard for the initial identification and evaluation of PNSTs and other soft tissue neoplasms [3, 4].

Radiologic identification of peripheral nerve enlargement raises a broad differential that includes benign peripheral nerve sheath tumors (BPNSTs), malignant peripheral nerve sheath tumors (MPNSTs), localized hypertrophic neuropathies, traumatic neuroma, and non-neurogenic malignancies such as neurolymphoma, perineural metastasis, and tumor mimics, such as vascular malformations, fibrolipoma, amyloid, and endometriosis [5–9]. BPNSTs are broadly classified as schwannomas (neuroleminomas), neurofibromas, or perineuriomas (Table 1). Schwannomas and neurofibromas are relatively common benign neoplasms of Schwann cell origin, each comprising ~ 5% of all benign soft tissue tumors [10]. Among these lesions, 95% arise sporadically while the remaining 5% arise in the setting of a neurocutaneous syndrome [10]. Perineuriomas, by comparison, are rare, arise from neoplastic perineurial cells, and are not associated with a neurocutaneous syndrome [11].

Confirmation of a neurogenic lesion limits the differential to spontaneously arising BPNSTs and MPNSTs, as well as PNSTs arising in the setting of a neurocutaneous syndrome such as neurofibromatosis types I (NF1) and II (NF2) or schwannomatosis [12]. Apart from size and invasiveness of the lesion, there are no reliable anatomic MRI features that help distinguish BPNSTs from MPNSTs and thus, MRI features do not preclude the necessity of biopsy for definitive diagnosis of MPNSTs [13]. Fluorine-18 fluorodeoxyglucose positron emission tomography (F18 FDG-PET) has been proposed to improve the diagnostic yield of BPNST versus MPNST; however, it is expensive, encompasses radiation, and both false positive and false negatives are not uncommon [14]. Therefore, its utility remains limited.

Diagnostic limitations of conventional MRI and F18 FDG-PET imaging have prompted investigation of MR diffusion contrast (i.e., DWI and DTI) that relies on characterizing the behavior of water molecules during diffusion-driven random displacement [15]. While DWI has been shown to provide information about tumor cellularity and necrosis [16], DTI is well suited for the evaluation of nerve microstructure by providing functional information about the direction and degree of diffusion as well as data about nerve orientation and integrity [17, 18]. DTI with fiber tractography appears particularly promising for the characterization of PNSTs. This article provides insights into the current perspectives of conventional MRI, DWI, and DTI in the diagnosis and management of such lesions. Future directions are also highlighted, including potential use of artificial intelligence approaches (radiomics) in the foreseeable future.

Conventional MRI techniques and MR neurography

Conventional MRI techniques involve the use of 2-dimensional (2D) T1-weighted (T1W) and T2-weighted (T2W) imaging, fat-suppressed T2W (fsT2W) imaging, and contrast-enhanced T1W image with fat suppression (CE-T1W) sequences for anatomic identification and lesion characterization [19]. The peri-lesional anatomy is best seen on T1W and tumor conspicuity is best seen on T2W imaging [20]. Multi-planar imaging reconstructions allow interrogation of the long axis of the nerve as well as the tumor, and CE-T1W interrogates tumor vascularity as well as cystic or hemorrhagic changes [21, 22]. Limitations of conventional MRI for PNST diagnosis include non-specific signal alterations on T1W and T2W images and variable contrast enhancement [21, 22]. Because the presence of fat within and around nerve structures significantly obscures pathologic signal intensity on T2W imaging, use of either frequency-selective fat saturation or short TI inversion recovery (STIR) sequences has become commonplace [23]. STIR improves the contrast-to-noise ratio (CNR) of soft tissue tumors by providing homogeneous fat signal suppression; however, it is more susceptible to degradation by motion and blood flow artifacts and usually results in lower signal-to-noise ratio (SNR) [24].

Simultaneous application of 2D methods with 3-dimensional (3D) non-selective MR neurography (MRN) sequences such as T2W spectral attenuated inversion recovery (SPAIR) and other variable turbo spin echo (TSE) sequences using variable flip angle evolutions allow better lesion localization and multi-planar isotropic tissue characterization than the 2D methods alone [25]. The MRN techniques continue to

Table 1 Imaging features of PNSTs and their clinical correlates. BPNSTs such as neurofibromas, schwannomas, and perineuriomas may be differentiated with moderate efficacy using conventional MR imaging features. Use of FDG-PET imaging and diffusion-weighted MR imaging may augment the diagnostic accuracy of MRI in classifying these tumors. Likewise, BPNSTs may be differentiated from MPNSTs using conventional MRI, FDG-PET, diffusion-weighted MRI, and accompanying clinical features.

Tumor identity	MR imaging appearance	SUV_{max} (F^{18} FDG-PET)	DWI and DTI	Clinical features
Neurofibroma	Split fat sign Target sign Fascicular sign Unencapsulated Often infiltration of the parent nerve Multi-fascicular involvement	Low (< 2–3)	Low diffusion restriction ADC > 1.3×10^{-3} mm/s^2 FA of parent nerve—reduced Tracts—partial disruption of tracts	Slow-growing Mild to moderate motor-sensory symptoms Can be either isolated or associated with NF1
Schwannoma	Split fat sign Fascicular sign Target sign Encapsulated Cystic changes, calcification, hemorrhage (ancient schwannoma) Eccentric to parent nerve One or two fascicular involvement in most cases Multi-fascicular involvement in segmental or plexiform schwanomatosis	Low (< 2–3) High SUV can be seen in schwannomatosis but malignancy is exceedingly rare	Low diffusion restriction ADC > $1.3–1.5 \times 10^{-3}$ mm/s^2 FA of parent nerve—reduced Tracts—nearly normal or partial disruption of tracts	Slow-growing Mild to moderate motor-sensory symptoms Can be either isolated or associated with NF2 or schwannomatosis
Perineurioma	Homogeneous and uniform fascicular enlargement and hyperintensity (honeycomb pattern) Lower limbs most common Multiple fascicles Can be associated with port wine stain (can mimic Klippel-Trènaunay-Weber syndrome)	Low (< 2–3)	Moderate diffusion restriction ADC > 1.1×10^{-3} mm/s^2 FA of parent nerve—reduced Tracts—nearly normal and/or thickened	Slow-growing Mild to moderate motor symptoms Isolated, not associated with a neurocutaneous syndrome
MPNST	Irregular or round shape Generally > 5 cm Peri-lesional edema Heterogeneous or peripheral enhancement Intra-tumoral necrosis/hemorrhage Peri-tumoral enhancement	High (> 3–4)	High diffusion restriction ADC < 1.1×10^{-3} mm/s^2 FA of parent nerve—reduced Tracts—partial high-grade or complete disruption of tracts	Rapidly growing New-onset pain or focal neurological deficit Either isolated or associated with NF1

evolve with multiple nerve-selective techniques now available on both 1.5 Tesla (T) and 3T platforms. These include 3D DW reversed fast imaging in steady-state free precession (PSIF), 3D T2W TSE Dixon, and nerve sheath signal increased with inked rest-tissue rapid acquisition of relaxation enhancement imaging (SHINKEI), which provide excellent nerve tissue CNR and fascicular details with effective vascular signal and background fat suppression [26]. Using these techniques, anatomic detail of the tumor and nerve can be generated at the fascicular level with sub-millimeter resolution, aiding in preoperative planning of PNSTs. MRN techniques can also be employed to identify post-operative tumor recurrence, which presents as a focal, irregular, nodular, hyperintense nerve enlargement or mass in the operated tumor bed with enhancement on CE-T1W [20].

Key MRI characteristics of PNSTs

The key MRI characteristics of BPNSTs, which can be seen with both neurofibromas and schwannomas, include the split fat sign, target sign, and fascicular sign [19, 21, 27]. Other features of benign status include absence of peripheral enhancement on CE-T1W and absence of peri-lesional edema [4]. Although neurofibromas and schwannomas cannot be reliably differentiated with conventional MRI, there are some features that may suggest one or the other. Neurofibromas are fusiform, unencapsulated, and locally or diffusely infiltrate the underlying nerve tissues. The fascicles of origin are usually non-functional [28]. On MRN, neurofibromas are usually associated with two or more fascicles entering and exiting the nerve (Fig. 1) [2, 28]. Treatment of a neurofibroma may

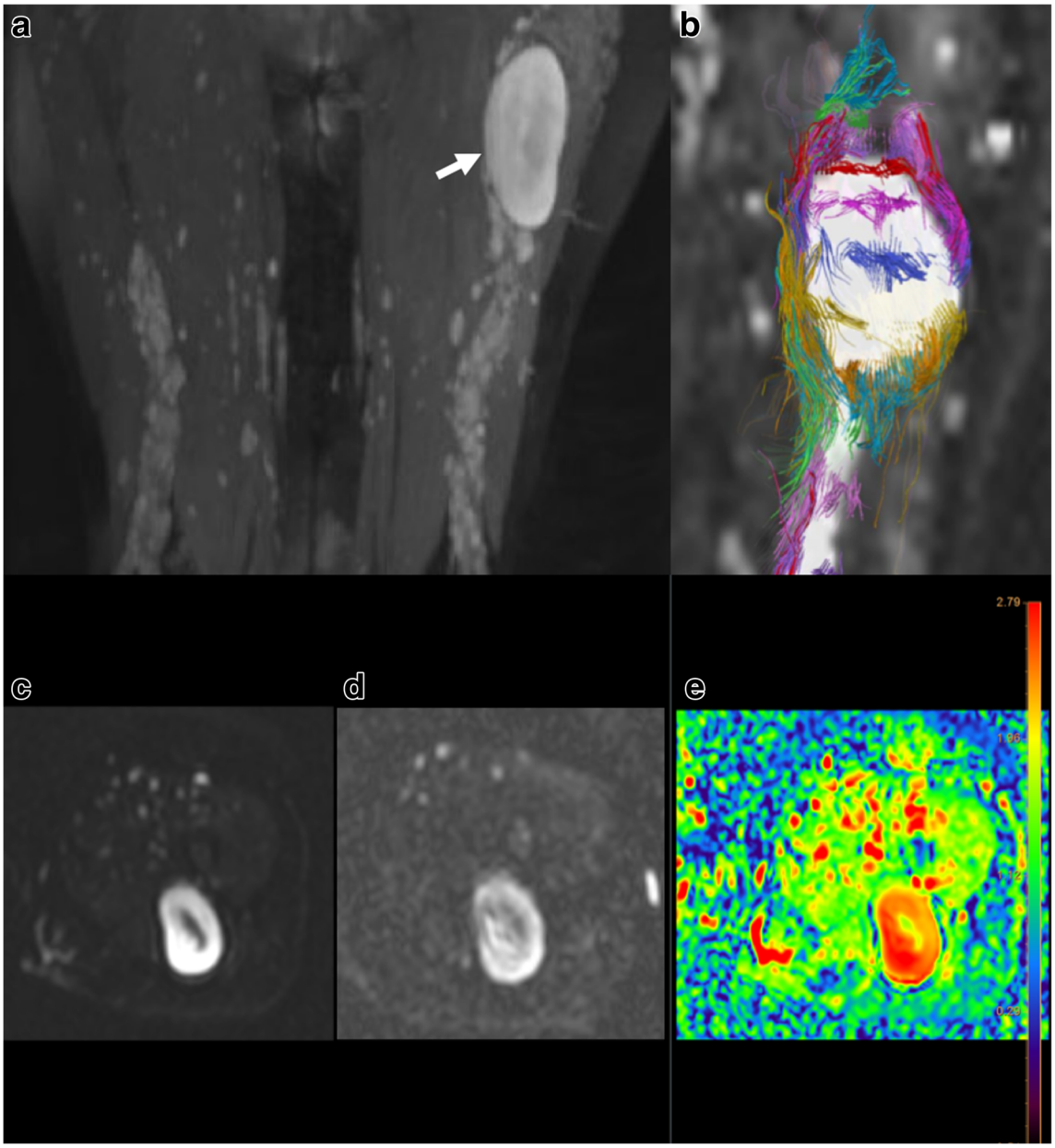

Fig. 1 Neurofibroma of the left posterior lateral thigh in a patient with known NF1. **a** Numerous PNSTs are seen along the sciatic nerves bilaterally on nerve selective MR neurography using 3D DW PSIF imaging along with a larger tumor. **b** Fiber tractography of the tumor from DTI reveals partially disrupted tracts splayed around and interspersed in the tumor. **c** Axial DTI ($b = 0$ s/mm^2) using 12 diffusion directions showing the target sign. **d** Axial DTI ($b = 600$ s/mm^2). **e** Colored MD map demonstrating high diffusivity with values measuring 2.1–2.7 × 10^{-3} mm^2/s. Red coloration represents areas of high diffusivity

involve either complete or partial resection of involved nerve segments, which can result in significant morbidity depending on the location of the lesion. Schwannomas, by comparison, present as an encapsulated mass positioned eccentrically to the nerve (Fig. 2). Although surgical enucleation of the mass with minimal damage to underlying nerve fascicles is theoretically possible, neurologic deficits and other post-operative complications are not uncommon [29].

MPNSTs are aggressive, locally infiltrative tumors with high metastatic potential and poor prognosis [1]. They differ from BPNSTs on MRI based on their larger diameter (> 5 cm), presence of peri-lesional edema (Fig. 3) and/or enhancement, peripheral enhancement with Gadolinium-based contrast agent, and intra-tumoral necrotic changes [4]. Presence of two or more of the aforementioned features in a neurogenic lesion indicates malignancy with 60% sensitivity and 90% specificity [3]. A problematic situation is often created by the presence of ancient schwannomas, as these lesions are large and can show cystic/hemorrhagic areas that mimic features of MPNSTs. Thus, biopsy is needed to confirm the diagnosis of MPNST.

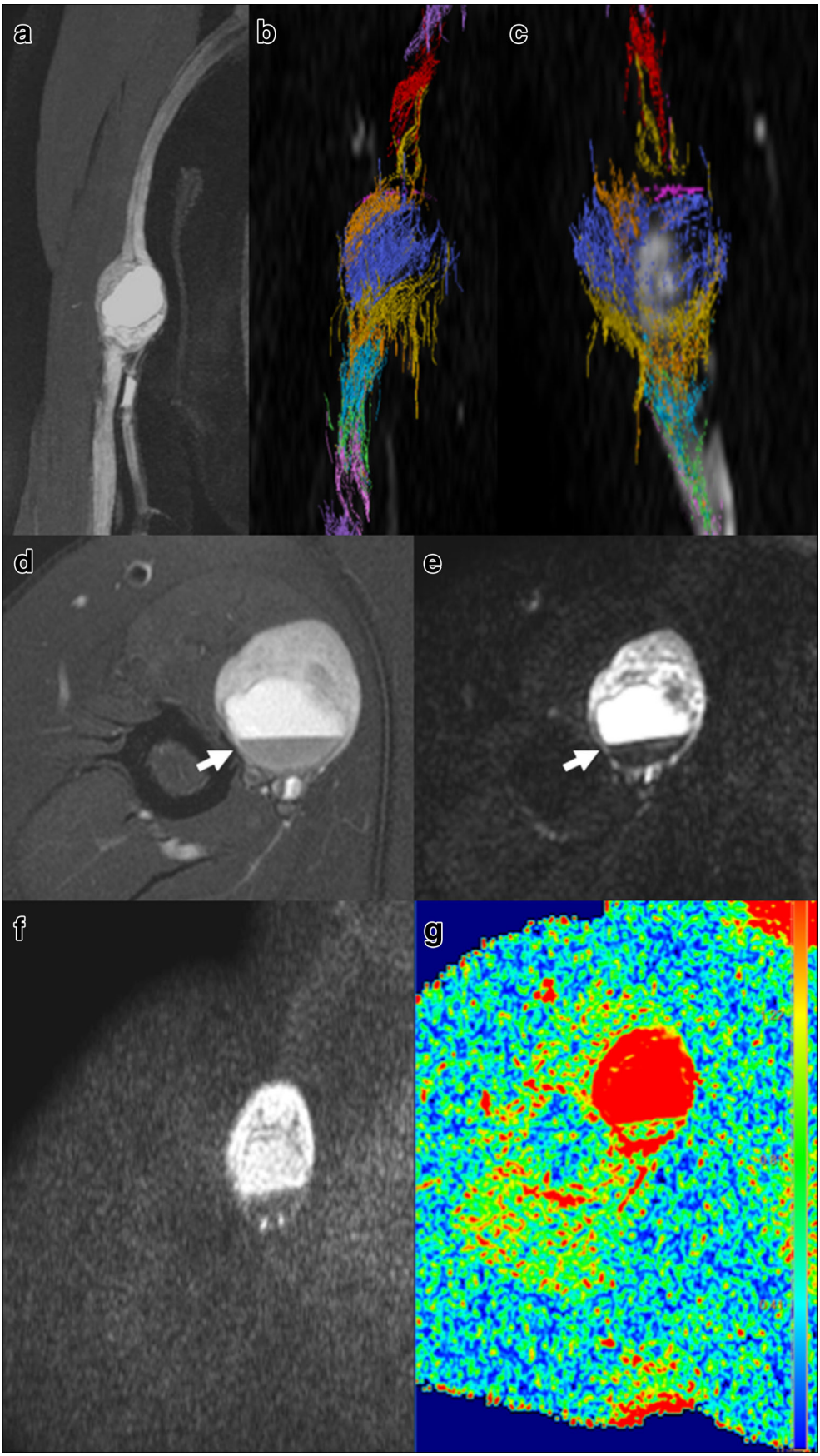

Fig. 2 Ancient schwannoma presenting as diffuse enlargement of the median nerve in the upper extremity. **a** Tumor conspicuity is readily visualized with 3D PSIF, along with central cystic changes. **b** DTI (0 s/mm^2) with fiber tractography demonstrating peripheral location of fascicles. **c** Fiber tractography reveals partial absence of tracts, splayed around the cystic area. **d**–**g** Axial T2 SPAIR (**d**), DTI (b = 0 s/mm^2) (**e**), DTI (b = 600 s/mm^2) (**f**), and colored MD map (**g**) show fluid level due to internal hemorrhage (arrows). MD values of 1.9 and 2.8×10^{-3} mm^2/s are seen in solid and cystic tumor regions, respectively, consistent with a benign lesion. Red and blue colorations represent areas of high and low diffusivity, respectively. FA of median nerve was reduced to 0.1–0.2, consistent with neuropathy

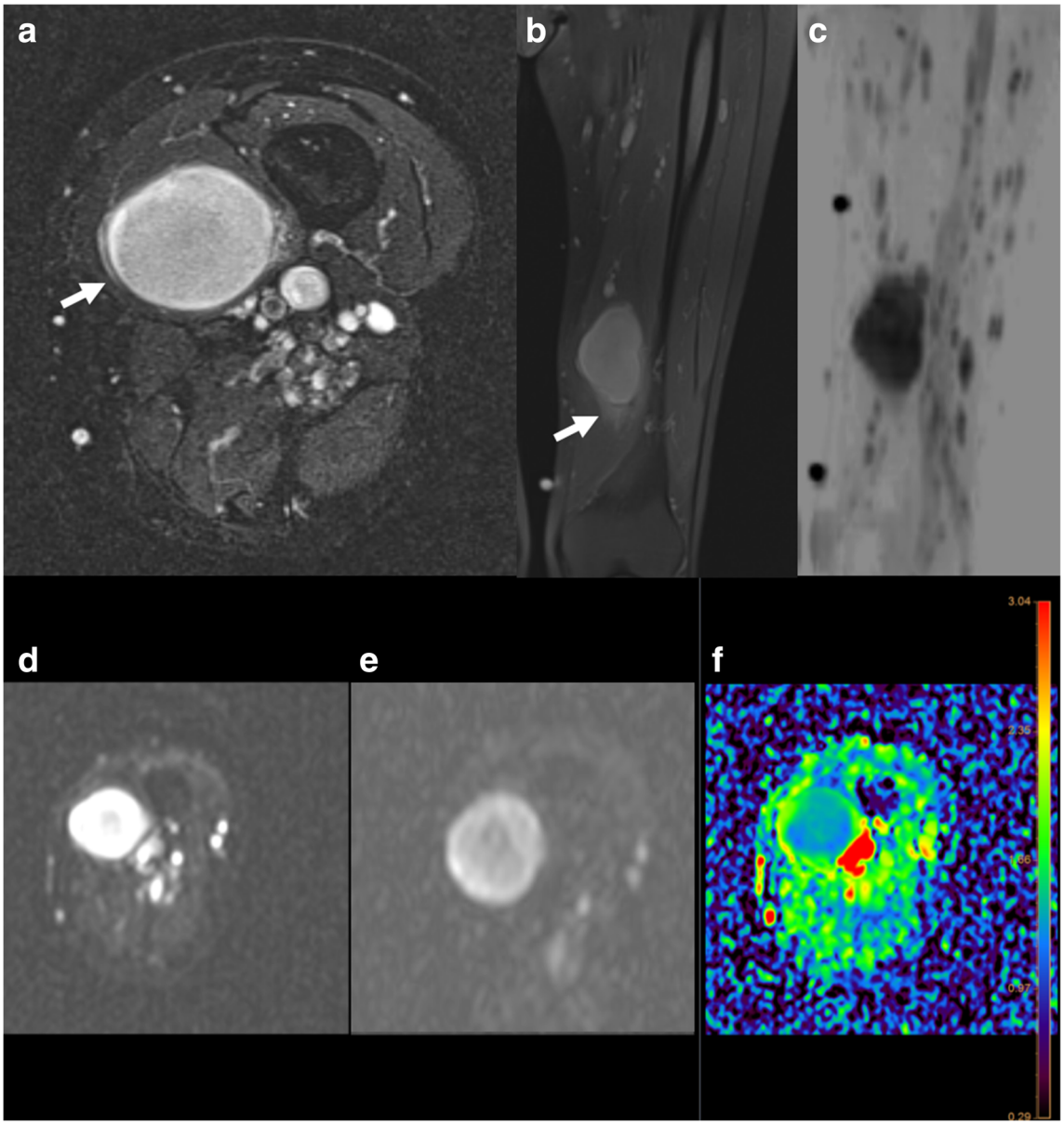

Fig. 3 MPNST of the left thigh. **a**, **b** Axial T2 SPAIR and coronal fat-saturated proton density weighted (fsPDW) show a dominant tumor in the vastus medialis and enlarged sciatic nerve in a known case of NF1. Also note mild peri-tumoral edema (arrows). **c** Inverted scale DWI maximum intensity projection (MIP) reveals innumerable smaller lesions besides the dominant lesion. **d**, **e** Axial DTI acquired at $b = 0$ s/mm^2 (**d**) and $b = 600$ s/mm^2 (**e**) b values. **f** Colored MD map demonstrates reduced diffusivity pattern of 1.0–1.2 × 10^{-3} mm^2/s. Red and blue colorations represent areas of high and low diffusivity, respectively

Diffusion-weighted MR imaging

An increasingly diverse array of diffusion-weighted MR imaging techniques has allowed invaluable diagnostic advances in the field of neuroimaging over the past two decades. The common theoretical framework for these techniques is built upon the physical principles of free molecular diffusion, described as the Brownian motion. In contrast, biological tissues are complex media which impose bounded domains that interfere with free diffusion, the most significant of which is the cell membrane [30].

In DWI, displacement along the axis of the diffusion gradient is visualized as attenuation of MR signal intensity. The opposite phenomenon is observed among highly cellular tissues, such as tumors, where there is greater restriction of free diffusion along the axis of the diffusion gradient, and consequently, high signal intensity.

A high ADC (> 1.0–1.1 × 10^{-3}) is generally reflective of benign nerve pathology, and is observed in neurofibroma as well as schwannoma, and other BPNSTs such as perineuriomas [5] (Fig. 4). Conversely, restricted diffusion and consequently low ADC (min. < 1.0–1.1 × 10^{-3}) is more often a feature of

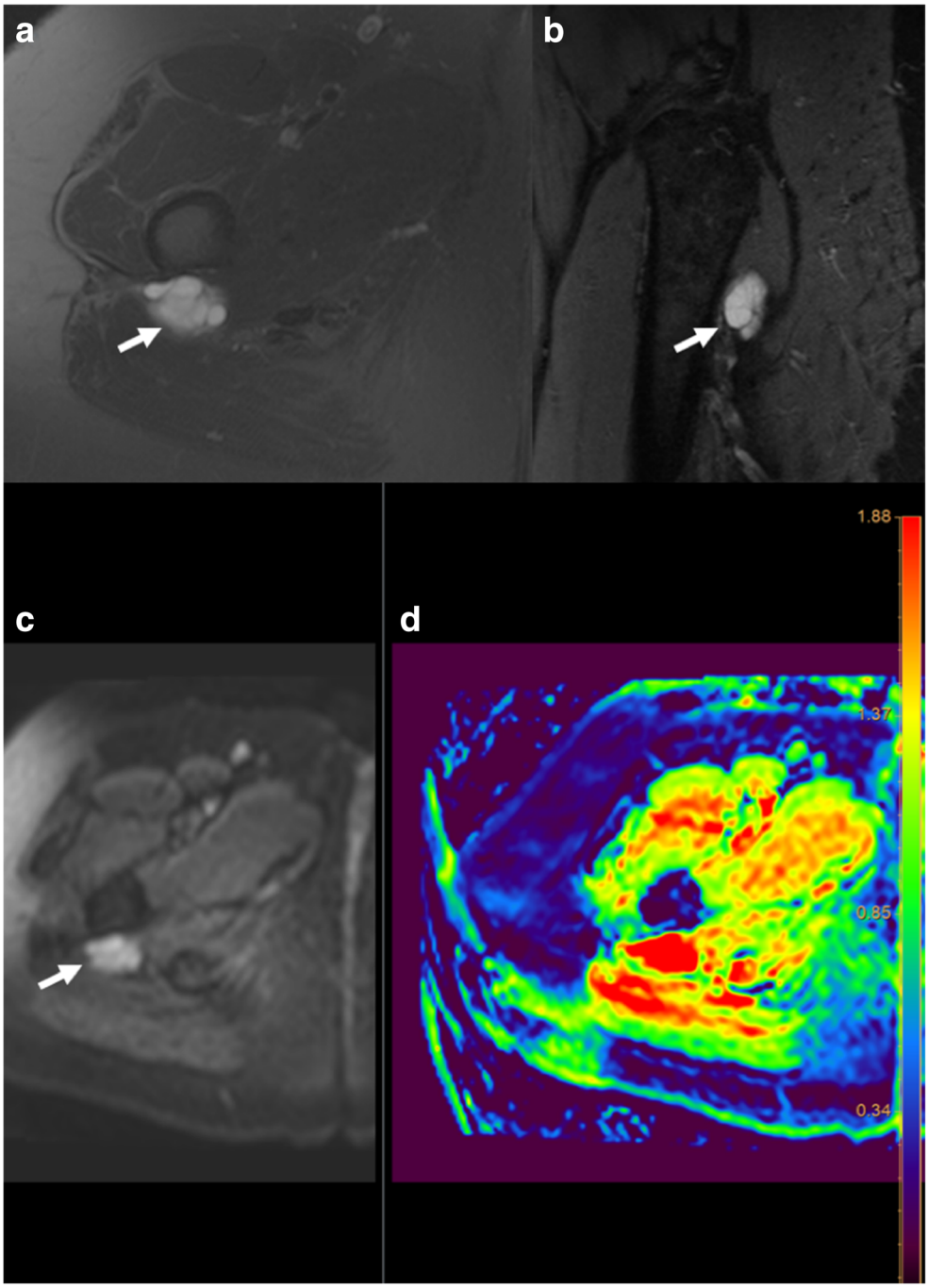

Fig. 4 Perineurioma of the right posteromedial thigh. **a**, **b** Axial T2 SPAIR and sagittal STIR images reveal a mass (arrows) with honeycomb pattern, classic for perineurioma. **c** DWI (b = 400 s/mm^2) and **d** colored ADC maps reveal high ADC = 1.9–2.0 × 10^{-3} mm^2/s, consistent with a benign lesion. Surgical histology revealed a myxoid perineurioma

malignancy [16]. It is important to consider the usefulness of DWI given evidence in the literature that a low ADC area should be re-biopsied if the initial biopsy result is negative for malignancy or is inconclusive. Furthermore, whole body MRI with DWI is an excellent screening technique to detect potentially malignant lesions which show worrisome features, such as heterogeneity on T2W or STIR imaging and/or exhibit diffusion restriction [5, 12].

Due to differences in the way manufacturers implement calculation of ADC, and inherent differences in water diffusion in human tissue compared to laboratory models used for ADC estimation, this technique suffers from certain limitations [31]. Although the ADC can provide valuable quantitative data concerning tissue diffusivity, it is sensitive to the effects of micro-capillary perfusion, also known as pseudodiffusivity [32]. Using multi-b value diffusion-weighted MR imaging, it is possible to differentiate the effects of diffusion and pseudodiffusion by interrogating parameters of intravoxel incoherent motion (IVIM) [33]. Because of their ability to characterize the

effects of capillary perfusion, IVIM surrogate imaging markers have been explored as a possible alternative to contrast enhancement for characterizing lesion vascularity in some tumors [33]. However, the application of these markers in the setting of PNSTs remains unexplored.

DWI does not provide directional information in the setting of anisotropic diffusion. DTI overcomes this limitation by sampling diffusion across six or more gradient directions, thereby allowing visualization of anisotropic diffusion across multiple axes simultaneously [34, 35]. Mean diffusivity [MD] is thought to be more useful than ADC in the domain of PNSTs due to larger number of directions in diffusion encoding [18]. The degree of anisotropy of a tissue is easily obtained through the calculation of fractional anisotropy [FA]. FA is indexed from 0 to 1, with FA = 0 representing free isotropic diffusion and FA = 1 representing complete anisotropy. The FA of pathologic nerves is usually lower than that which is seen in healthy contralateral nerves, possibly reflecting myelin loss and/or axonal degeneration of involved nerve segments [18].

Fiber tractography can be used to accurately delineate healthy and pathologic fascicles in most PNSTs, as well as in the setting of other PNS pathologies [17, 36]. Tract disruption is often more severe in MPNSTs than BPNSTs, with BPNSTs usually exhibiting a near normal appearance and partial rather than complete tract disruption [17, 18]. The treatment goal for most PNSTs is gross total resection with neural preservation; however, there is often considerable difficulty in the intra-operative delineation of healthy and pathologic nerve tissues [37]. Pre-operative visualization of the fascicular course and integrity using fiber tractography is therefore likely to be of great value for surgical planning and subsequent preservation of existing nerve function following tumor resection. In a preliminary study by Schmidt M et al [17], there was good correlation of pre-operative fascicular visualization and intra-operative anatomy. The authors did not attempt correlation of DTI measurements of different areas of neural topography with intra-operative electrophysiology to define fascicular involvement and function, which can be a subject of future research using this novel technique. In median nerves, the optimization of reconstruction parameters for fiber tractography on echo planar imaging is best achieved at a *b* value of 1200 s/mm^2, with a maximum angulation tolerance of 10 degrees and minimum FA threshold of 0.2 [38]. Reproducibility of tractography, anisotropy, and diffusivity, however, remains a challenge even in healthy subjects without disease, when the peripheral nerve (lumbosacral nerve roots) DTI is obtained after an interval, as recently shown by Haakma W et al [39]. Nevertheless, DTI tractography remains a work in progress, with a recent study showing improved tractography and less image distortion using single-shot spin echo sequences as compared to echo planar imaging in the domain of lumbar nerve root evaluation [40].

Future directions

DTI seems promising in the domain of PNST diagnosis, preoperative planning, and characterization. Augmentation of diagnostic accuracy has been shown in peripheral neuropathy [41]. However, no large efforts have yet been undertaken to classify peripheral nerve tumors based on parameters of diffusivity, or to corroborate these markers using histology, electrophysiology, and intravenous contrast perfusion imaging. Scientific studies are relatively lacking in demonstrating the utility of these techniques in correlation of nerve function with the size or type of tumor. While newer methods of exploiting DWI and DTI are available including multi-shot DTI, kurtosis, and histogram analysis, more research is needed to demonstrate their efficacy [42]. Limitations in DTI mapping, such as an inability to resolve more than a single fiber orientation, may soon be overcome by employment of techniques like q-ball imaging, which provide enhanced angular resolution in lesions with tortuously coursing fascicles and multiple fiber directions [43, 44]. New MRN methods such as SHINKEI quant or 3D T2W TSE Dixon quant are becoming available for T2 mapping during nerve-selective neurography, and may be useful to distinguish different tumor types quantitatively [45].

Beyond the realm of MR technologies, the advent of artificial intelligence-directed radiomics and high-throughput image mining promises to reveal new imaging signatures that will augment or, perhaps, supersede current diagnostic models in oncology [46]. Radiomics refers to the automated quantification of a radiographic phenotype. It uses computerized approaches for generation of a convolutional neural network, initial machine learning followed by validation and evaluation of test data sets. Many quantitative measures, also known as radiomic measures, such as intensity, shape, texture, wavelet, and LOG features, are extracted by the machine from the image data sets. Using deep learning methods and multi-order statistics to one or more MRI sequences in isolation and/or combination, many diagnostic, predictive, or prognostic imaging markers can be derived. In our recent evaluation of benign versus malignant soft tissue musculoskeletal tumors using simple T2W imaging, 85–90% accuracy was achieved using radiomics for multiple geometric and textural pathologic features (work under review). We also compared the accuracy of radiomic analysis to the accuracy of expert radiologists, and the former exceeded reader diagnostic capability. Computational approaches such as these are expected to improve diagnostic confidence among radiologists and can uncover quantitative imaging characteristics that fail to be appreciated by the naked eye. If one could differentiate schwannoma from neurofibroma, the automated approach of radiomics could substantially aid pre-surgical planning and assist in patient management and prognostication.

Conclusion

To summarize, diffusion imaging augments the moderate diagnostic utility of conventional MR imaging. As newer functional MR technologies and software approaches become increasingly familiar and available, it is likely that their utility will continue to expand outward beyond applications in the central nervous system to improve the diagnosis and management of PNSTs.

Funding The authors state that this work has not received any funding.

Compliance with ethical standards

Guarantor The scientific guarantor of this publication is Avneesh Chhabra, MD.

Conflict of interest The authors of this manuscript declare relationships with the following companies: AC receives royalties from Jaypee and Wolters. AC also serves as consultant with ICON Medical.

The remaining authors declare that they have no conflicts of interest.

Statistics and biometry No complex statistical methods were necessary for this paper.

Informed consent For this type of study, formal consent is not required.

Ethical approval Institutional Review Board approval was obtained.

Study subjects or cohorts overlap One study subject has been previously reported in AJNR News Digest, May–June 2017, but the images submitted herein are different from those submitted in that digest.

Methodology
- Retrospective
- Observational
- Performed at one institution

References

1. Bernthal NM, Putnam A, Jones KB, Viskochil D, Randall RL (2014) The effect of surgical margins on outcomes for low grade MPNSTs and atypical neurofibroma. J Surg Oncol 110(7):813–816
2. Kim DH, Murovic JA, Tiel RL, Moes G, Kline DG (2005) A series of 397 peripheral neural sheath tumors: 30-year experience at Louisiana State University Health Sciences Center. J Neurosurg 102(2):246–255
3. Wasa J, Nishida Y, Tsukushi S et al (2010) MRI features in the differentiation of malignant peripheral nerve sheath tumors and neurofibromas. AJR Am J Roentgenol 194(6):1568–1574
4. Soldatos T, Fisher S, Karri S, Ramzi A, Sharma R, Chhabra A (2015) Advanced MR imaging of peripheral nerve sheath tumors including diffusion imaging. Semin Musculoskelet Radiol 19:179–190
5. Ahlawat S, Chhabra A, Blakely J (2014) Magnetic resonance neurography of peripheral nerve tumors and tumorlike conditions. Neuroimaging Clin N Am 24(1):171–192
6. Wilson TJ, Howe BM, Stewart SA, Spinner RJ, Amrami KK (2017) Clinicoradiological features of intraneural perineuriomas obviate the need for tissue diagnosis. J Neurosurg 1:1–7. https://doi.org/10.3171/2017.5.JNS17905.
7. Beaman FD, Kransdorf MJ, Menke DM (2004) Schwannoma: radiologic-pathologic correlation. Radiographics 24(5):1477–1481
8. Yilmaz S, Ozolek JA, Zammerilla LL, Fitz CR, Grunwaldt LJ, Crowley JJ (2014) Neurofibromas with imaging characteristics resembling vascular anomalies. AJR Am J Roentgenol 203(6): W697–W705
9. Broski SM, Johnson GB, Howe BM et al (2016) Evaluation of (18)F-FDG PET and MRI in differentiating benign and malignant peripheral nerve sheath tumors. Skeletal Radiol 45(8):1097–1105
10. Kransdorf MJ (1995) Benign soft-tissue tumors in a large referral population: distribution of specific diagnoses by age, sex, and location. AJR Am J Roentgenol 164(2):395–402
11. Restrepo CE, Amrami KK, Howe BM, Dyck PJB, Mauermann ML, Spinner RJ (2015) The almost-invisible perineurioma. Neurosurg Focus 39(3):E13. https://doi.org/10.3171/2015.6.FOCUS15225
12. Ahlawat S, Fayad LM, Khan MS et al (2016) Current whole-body MRI applications in the neurofibromatoses. Neurology 87(7 Suppl 1):S31–S39
13. Karsy M, Guan J, Ravindra VM, Stilwill S, Mahan MA (2016) Diagnostic quality of magnetic resonance imaging interpretation for peripheral nerve sheath tumors: can malignancy be determined? J Neurol Surg A Cent Eur Neurosurg 77(6):495–504
14. Shahid KR, Amrami KK, Esther RJ, Lowe VJ, Spinner RJ (2011) False-negative fluorine-18 fluorodeoxyglucose positron emission tomography of a malignant peripheral nerve sheath tumor arising from a plexiform neurofibroma in the setting of neurofibromatosis type 1. J Surg Orthop Adv 20(2):132–135
15. Hagmann P, Jonasson L, Maeder P, Thiran JP, Wedeen VJ, Meuli R (2006) Understanding diffusion MR imaging techniques: from scalar diffusion-weighted imaging to diffusion tensor imaging and beyond. Radiographics 26(suppl 1):S205–S223
16. Demehri S, Belzberg A, Blakeley J, Fayad LM (2014) Conventional and functional MR imaging of peripheral nerve sheath tumors: initial experience. AJNR Am J Neuroradiol 35(8): 1615–1620
17. Schmidt M, Kasprian G, Amann G, Duscher D, Aszmann OC (2015) Diffusion tensor tractography for the surgical management of peripheral nerve sheath tumors. Neurosurg Focus 39(3):E17
18. Chhabra A, Thakkar RS, Andreisek G et al (2013) Anatomic MR imaging and functional diffusion tensor imaging of peripheral nerve tumors and tumorlike conditions. AJNR Am J Neuroradiol 34(4): 802–807
19. Kransdorf MJ, Murphey MD (2000) Radiologic evaluation of soft-tissue masses: a current perspective. AJR Am J Roentgenol 175(3): 575–587
20. Singh T, Kliot M (2007) Imaging of peripheral nerve tumors. Neurosurg Focus 22(6):1–10
21. Wu JS, Hochman MG (2009) Soft-tissue tumors and tumorlike lesions: a systematic imaging approach. Radiology 253(2):297–316
22. Nandigam K, Mechtler LL, Smirniotopoulos JG (2014) Neuroimaging of neurocutaneous diseases. Neurol Clin 32(1): 159–192
23. Tokuda O, Harada Y, Matsunaga N (2009) MRI of soft-tissue tumors: fast STIR sequence as substitute for T1-weighted fat-suppressed contrast-enhanced spin-echo sequence. AJR Am J Roentgenol 193(6):1607–1614
24. Rubin DA, Kneeland JB (1994) MR imaging of the musculoskeletal system: technical considerations for enhancing image quality and diagnostic yield. AJR Am J Roentgenol 163(5):1155–1163
25. Viallon M, Vargas MI, Jlassi H, Lövblad KO, Delavelle J (2008) High-resolution and functional magnetic resonance imaging of the brachial plexus using an isotropic 3D T2 STIR

(short term inversion recovery) SPACE sequence and diffusion tensor imaging. Eur Radiol 18(5):1018–1023
26. Hiwatashi A, Togao O, Yamashita K et al (2017) Lumbar plexus in patients with chronic inflammatory demyelinating polyneuropathy: evaluation with 3D nerve-sheath signal increased with inked rest-tissue rapid acquisition of relaxation enhancement imaging (3D SHINKEI). Eur J Radiol 93:95–99
27. Murphey MD, Smith WS, Smith SE, Kransdorf MJ, Temple HT (1999) From the archives of the AFIP imaging of musculoskeletal neurogenic tumors: radiologic-pathologic correlation. Radiographics 19(5):1253–1280
28. Levi AD, Ross AL, Cuartas E, Qadir R, Temple HT (2010) The surgical management of symptomatic peripheral nerve sheath tumors. Neurosurgery 66(4):833–840
29. Kim SM, Seo SW, Lee JY, Sung KS (2012) Surgical outcome of schwannomas arising from major peripheral nerves in the lower limb. Int Orthop 36(8):1721–1725
30. Beaulieu C (2002) The basis of anisotropic water diffusion in the nervous system - a technical review. NMR Biomed 15(7–8):435–455
31. Bourne RM (2015) The trouble with apparent diffusion coefficient papers. J Med Radiat Sci 62(2):89–91
32. LeBihan D, Breton E, Lallemand D, Grenier P, Cabanis E, Laval-Jeantet M (1986) MR imaging of intravoxel incoherent motions: application to diffusion and perfusion in neurologic disorders. Radiology 161(2):401–407
33. Sigmund EE, Cho GY, Kim S et al (2011) Intravoxel incoherent motion imaging of tumor microenvironment in locally advanced breast cancer. Magn Reson Med 65(5):1437–1447
34. Mori S, Zhang J (2006) Principles of diffusion tensor imaging and its applications to basic neuroscience research. Neuron 51(5):527–539
35. Basser PJ, Mattiello J, LeBihan D (1994) MR diffusion tensor spectroscopy and imaging. Biophys J 66:93–108
36. Vargas MI, Viallon M, Nguyen D, Beaulieu JY, Delavelle J, Becker M (2010) New approaches in imaging of the brachial plexus. Eur J Radiol 74(2):403–410
37. Desai KI (2017) The surgical management of symptomatic benign peripheral nerve sheath tumors of the neck and extremities: an experience of 442 cases. Neurosurgery 81(4):568–580
38. Guggenberger R, Eppenberger P, Markovic D et al (2012) MR neurography of the median nerve at 3.0 T: optimization of diffusion tensor imaging and fiber tractography. Eur J Radiol 81(7):e775–e782
39. Haakma W, Hendrikse J, Uhrenholt L et al (2018) Multicenter reproducibility study of diffusion MRI and fiber tractography of the lumbosacral nerves. J Magn Reson Imaging. https://doi.org/10.1002/jmri.25964
40. Sakai T, Doi K, Yoneyama M, Watanabe A, Miyati T, Yanagawa N (2018) Distortion-free diffusion tensor imaging for evaluation of lumbar nerve roots: utility of direct coronal single-shot turbo spin-echo diffusion sequence. Magn Reson Imaging 49:78–85
41. Bäumer P, Pham M, Ruetters M et al (2014) Peripheral neuropathy: detection with diffusion-tensor imaging. Radiology 273(1):185–193
42. Wagner MW, Narayan AK, Bosemani T, Huisman TA, Poretti A (2016) Histogram analysis of diffusion tensor imaging parameters in pediatric cerebellar tumors. J Neuroimaging 26(3):360–365
43. Tuch DS (2004) Q-ball imaging. Magn Reson Med 52(6):1358–1372
44. Tuch DS, Reese TG, Wiegell MR, Wedeen VJ (2003) Diffusion MRI of complex neural architecture. Neuron 40:885–895
45. Hiwatashi A, Togao O, Yamashita K et al (2018) Lumbar plexus in patients with chronic inflammatory demyelinating polyradiculoneuropathy: evaluation with simultaneous T2 mapping and neurography method with SHINKEI. Br J Radiol 48:20180501. https://doi.org/10.1259/bjr.20180501
46. Lambin P, Leijenaar RTH, Deist TM et al (2017) Radiomics: the bridge between medical imaging and personalized medicine. Nat Rev Clin Oncol 14(12):749–762